CHINA FOUNDRY Research & Development
Vol. 23 No. 3 May 2026
www.springer.com/41230
https://doi.org/10.1007/s41230-026-5243-x

Factors influencing high-temperature compressive strength of alkaline phenolic resin-bonded sand

Xin Peng[1], Yu-yang Qi[1], Peng Yu[1], Peng Wan[1, 2], Zhen-wei Liu[1], Wen Li[1], Xu Shen[1], Xiao-yuan Ji[1], *Ya-jun Yin[1], Yuan-cai Li[1], and Jian-xin Zhou[1]

1. State Key Laboratory of Materials Processing and Die & Mould Technology, Huazhong University of Science & Technology, Wuhan 430074, China

2. School of Mechanical & Electrical Engineering, Wuhan Institute of Technology, Wuhan 430205, China

Abstract: During the casting process, no-bake resin-bonded sand molds and cores rapidly heat up upon contact with high-temperature molten metal, causing dramatic changes in the resin binder system and a significant deterioration in mechanical properties, which subsequently leads to casting defects. To reveal the mechanism behind the evolution of high-temperature performance, the effects of resin content, base sand type, and particle size on the compressive strength of alkaline phenolic no-bake resin-bonded sand at temperatures ranging from 600 °C to 1,000 °C were investigated. The results show that the temperature range of 600–800 °C represents the primary stage of strength loss, corresponding to intense resin decomposition. Meanwhile, structural reorganization of the carbon skeleton above 900 °C can lead to a partial recovery of strength. This study provides key data and theoretical support for understanding the high-temperature mechanical behavior of resin-bonded sand and its relationship with casting defects.

Keywords: no-bake resin-bonded sand; alkaline phenolic resin; high temperature strength; resin content; base sand; AFS fineness number

CLC numbers: TG221^{+}.1 **Document code:** A **Article ID:** 1672-6421(2026)03-336-09

1 Introduction

Sand casting is one of the key forming processes for producing large-scale metal components with complex geometries, reliable quality, and cost-effectiveness[1-6]. Among various sand casting processes, no-bake resin-bonded sand technology has held a dominant position in molding and core making over the past decades[7, 8] due to its advantages such as high molding efficiency and good dimensional stability[9-11]. The fundamental principle of this process involves the uniform mixing of base sand, resin, and a curing agent. In this mixture, the resin undergoes a curing agent-catalyzed cross-linking reaction, coating the sand particles and forming robust resin bridges. This network of bonded sand particles constructs molds or cores with sufficient mechanical strength for foundry applications.

***Ya-jun Yin**

Male, born in 1985, Associate Professor, and Doctoral Supervisor. Research interest: Numerical simulation of casting.

E-mail: yinyajun436@hust.edu.cn

Received: 2025-10-07; Revised: 2026-02-08; Accepted: 2026-04-09

During pouring, the resin-bonded molds (and cores) come into direct contact with high-temperature molten metal. The resin binder system undergoes a series of complex physicochemical changes under high temperatures (typically exceeding 1,200 °C[12, 13]) and in an oxygen-deficient environment[14-16], leading to significant alterations in mechanical properties. When molten metal first contacts the sand mold, an ideal thermal contact exists between them. At this moment, the sensible heat of the liquid metal is rapidly released into the surface layer of the sand mold. During this stage, the interfacial heat transfer coefficient reaches its historical peak. Studies indicate that for preheated sand molds or those with specific coatings, the initial heat transfer coefficient can reach several thousand $W \cdot m^{-2} \cdot K^{-1}$, owing to the maximized direct contact area at solid-solid or liquid-solid interfaces. Such instantaneous high-intensity heat flux causes the temperature of the sand mold's surface layer to rise to approximately 1,000 °C within a fraction of a second[17, 18]. This may subsequently induce casting defects such as hot tearing and veining, which are closely related to the high-temperature strength of the molds[19]. Therefore, a systematic

evaluation of the mechanical behavior of no-bake resin-bonded sand under high-temperature conditions is of considerable engineering significance. It not only facilitates an in-depth understanding of its service performance but also provides a scientific basis for the rational selection of base sand type, particle size distribution, and resin content in actual production.

However, current research on the high-temperature mechanical properties of no-bake resin-bonded sand remains significantly limited. Firstly, most studies focus on the residual strength of the materials[20], that is, the strength measured after the specimen is heated to high temperatures and subsequently cooled to room temperature, while failing to directly measure its strength at elevated temperatures. Consequently, it is difficult to accurately reflect the actual mechanical behavior of resin-bonded sand during the pouring process. Secondly, even though a few studies have attempted high-temperature strength testing, the temperature range is generally below 500 °C, far below the high-temperature conditions that molds experience in actual casting processes. This makes the relevant data inadequate for effectively guiding process design in high-temperature intervals.

Although some studies have explored the performance evolution of resins and their pyrolysis products over relatively wide temperature ranges[21–23], current research on resin-bonded sand systems remains primarily concentrated in the low- to medium-temperature range. Ratke et al.[24] measured both bending and compressive strengths to investigate the effects of grain size and binder content on molding sand. Dobosz et al.[25] studied the bending strength of no-bake furan resin sand at room temperature and its thermal deformation up to 450 °C. Stauder et al.[26] systematically compared the effects of four different binders and various storage periods on the room-temperature properties of sand cores. Ghosh et al.[27] tested both the high-temperature strength of resin-bonded sand at 450 °C and its residual strength after cooling. Furthermore, González et al.[28] investigated the influence of binder type and resin content on material properties within the range of room temperature to 150 °C. Bargaoui et al.[14] analyzed the mechanical behavior of sand cores and binder resins within the range of room temperature to 450 °C. In general, there is a lack of systematic understanding regarding the mechanical behavior of resin-bonded sand, particularly the direct evolution of high-temperature strength, at temperatures above 500 °C.

Therefore, the present study focuses on no-bake alkaline phenolic resin-bonded sand (APRBS) and systematically investigates the evolution of its compressive strength within the high-temperature range of 600–1,000 °C. It specifically examines the influencing mechanisms of three key factors, resin content, base sand type, and base sand particle size, on the high-temperature mechanical properties of materials. The research aims to deepen the understanding of the strength degradation of resin-bonded sand during the casting process and to provide reliable data support and theoretical guidance for the design and process optimization of sand molds in actual production.

2 Materials and methods

2.1 Base sand

To examine the effect of base sand type on the high-temperature compressive strength of alkaline phenolic resin-bonded sand, three kinds of base sand, namely, Dalin standard sand (DL sand), Zhangzhou sand (ZZ sand), and spherical ceramic sand (SC sand), were selected for sample preparation. Their compositions are listed in Table 1.

Table 1: Compositions of the three kinds of base sand (wt.%)

Sand type	SiO_2	Al_2O_3	H_2O	CaO+MgO	Fe_2O_3
DL sand	≥92	<4.5	<0.30	<0.4	<0.3
ZZ sand	≥97	<1.0	<0.01	<0.2	<0.2
SC sand	15–22	65–82	<0.10	-	-

To investigate the influence of grain size distribution, specimens were prepared using DL sand with three different mesh numbers: 40/70, 50/100, and 70/140. The American Foundry Society (AFS) fineness number, referenced from the Chinese standard GB/T 9442-2010 [Eq. (1)], was adopted as the quantitative measure of grain size for subsequent analysis.

$$\eta = \frac{\Sigma P_n X_n}{\Sigma P_n} \tag{1}$$

where η is the average fineness of the raw sand sample, P_n is the percentage by mass of raw sand retained on sieve n relative to the total sample mass, X_n is the fineness factor, and n is the sieve number.

2.2 Alkaline phenolic resin and curing agent

Alkaline phenolic resin (APR) was used as the binder for the resin-bonded sand. Both the resin and the curing agent were supplied by Suzhou Xingye Materials Technology Co., Ltd., and their key parameters are listed in Table 2.

In order to investigate the influence of resin content on the high-temperature compressive strength, three different resin addition ratios were designed, with the specific compositions detailed in Table 3.

Table 2: Characteristics of alkaline phenolic resin and its curing agent

Material	Density (25 °C, g·cm^{-3})	Viscosity (25 °C, mPa·s)	Free formal-dehyde (%)
Alkaline phenolic resin	1.2–1.3	≤150	≤0.1
Curing agent	1.0–1.2	≤30	-

Table 3: Alkaline phenolic resin-bonded sand with three different mass ratios of resin

APR sand notation	Base sand: resin: curing agent	Resin (wt.%)
APR1	1000: 12: 2.4	1.2
APR2	1000: 15: 3.0	1.5
APR3	1000: 20: 4.0	2.0

2.3 Specimen preparation and strength test

The specimen preparation process for the resin-bonded sand was as follows: First, the base sand and the curing agent were uniformly mixed. Then, the alkaline phenolic resin was added and mixing continued until a homogeneous mixture was achieved. Subsequently, the mixture was placed into a specialized mold. After reaching the designated demolding time, the specimens were demolded and stored in a constant temperature and humidity environment (20 °C, 35% RH) for 24 h prior to the high-temperature compressive strength test. A flowchart illustrating the preparation process can be seen in Fig. 1.

The specimens were fabricated using a hollow cylindrical mold independently developed by the research team and protected under a patent[28]. Compared to solid specimens, the hollow structure enables more uniform heating throughout the specimen cross-section during high-temperature exposure. This design mitigates the measurement inaccuracies caused by thermal gradients in solid specimens, thereby providing a more accurate representation of the material's strength characteristics at the target temperature. A schematic diagram illustrating the structural advantage of the hollow specimen is presented in Fig. 2. This design minimizes the through-thickness thermal gradient present in solid cylinders during rapid heating.

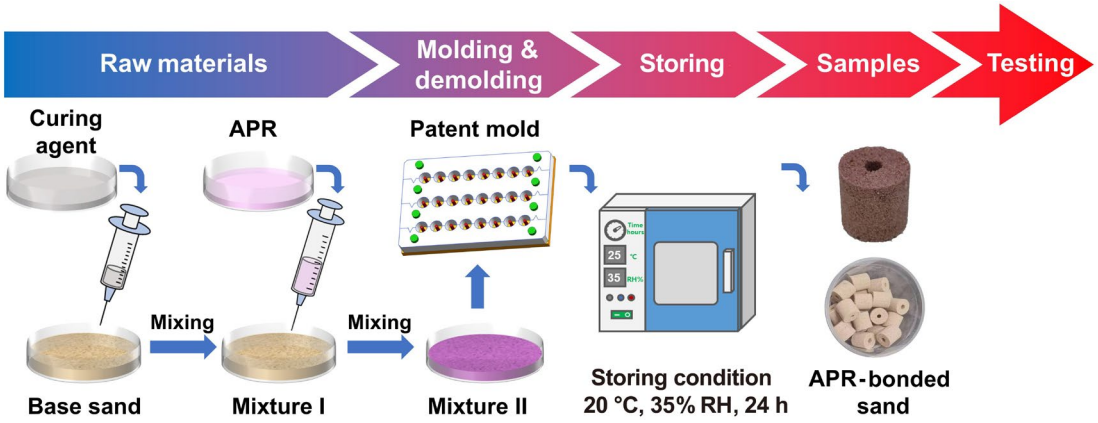

Fig. 1: Flowchart of the sample preparation process

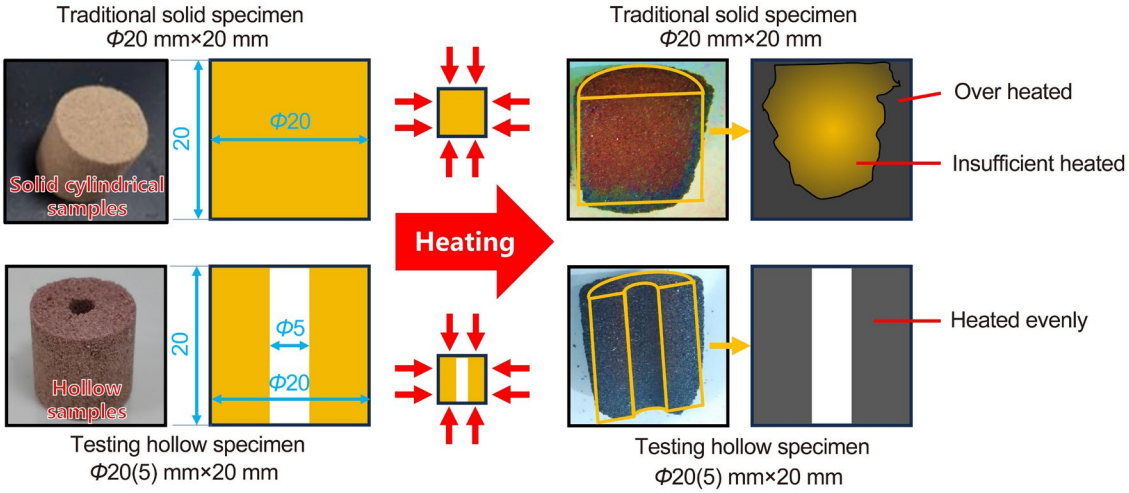

Fig. 2: Structural advantage of hollow specimen

Based on the aforementioned methods, this study systematically prepared alkaline phenolic no-bake resin-bonded sand specimens with varying resin contents, base sand types, and particle sizes. The high-temperature compressive strength of these specimens was tested within the range of 600–1,000 °C. During testing, the specimens were subjected to compression experiments immediately after being heated to the predetermined temperature. Each experimental group was repeated eight times, and the results are expressed as the mean value.

3 Results and discussion

3.1 Resin content

As shown in Figs. 3(a) and (b), the compressive strength of alkaline phenolic resin-bonded sand (prepared with 50/100 DL sand) exhibits a staged decline as temperature increases. In the temperature range of 600 °C–800 °C, specimens with three different resin contents all show significant strength reduction, which is primarily attributed to the intensive thermal decomposition of the resin matrix. When the temperature rises

above 800 °C, the rate of strength loss slows noticeably, particularly within the 800 °C–900 °C interval, the strength of the samples stabilizes, indicating that resin pyrolysis is largely complete and the resulting initial amorphous carbon structure provides a certain degree of thermal stability to the material. To further illustrate this point, the TG/DTG experimental results are cited from our previous study[29] on alkaline phenolic resin, as shown in Fig. 4.

It can be observed in Fig. 3(a) that over the entire temperature range, the high-temperature strength of the specimens generally increases with an increase in resin content. The strength variation trends of APR2 and APR3 are highly similar, suggesting that once the resin content reaches a certain level, its further increases contribute diminishing returns to strength enhancement. The strength curve of APR1 is significantly lower than those of APR2 and APR3 below 800 °C, likely due to its lower resin content, which is insufficient to fully coat the sand particles and form an adequate number and quality of resin bridges, resulting in reduced load-bearing capacity at high temperatures. Above 800 °C, as the resin in APR1 has already decomposed completely at an earlier stage, its strength stabilizes, showing a different trend compared to specimens with higher resin contents.

Figure 3(b) further reveals the characteristics of strength loss across different temperature intervals. For both APR2 and APR3, the most significant strength loss occurs in the temperature ranges of 600–700 °C and 700–800 °C, which is closely related to the main chain scission and thermal decomposition behavior of the resin within these temperature intervals. In the temperature range of 800–900 °C, strength loss in all specimens decreases to its lowest level, indicating that resin pyrolysis is essentially complete and the material has entered the carbon residue stage.

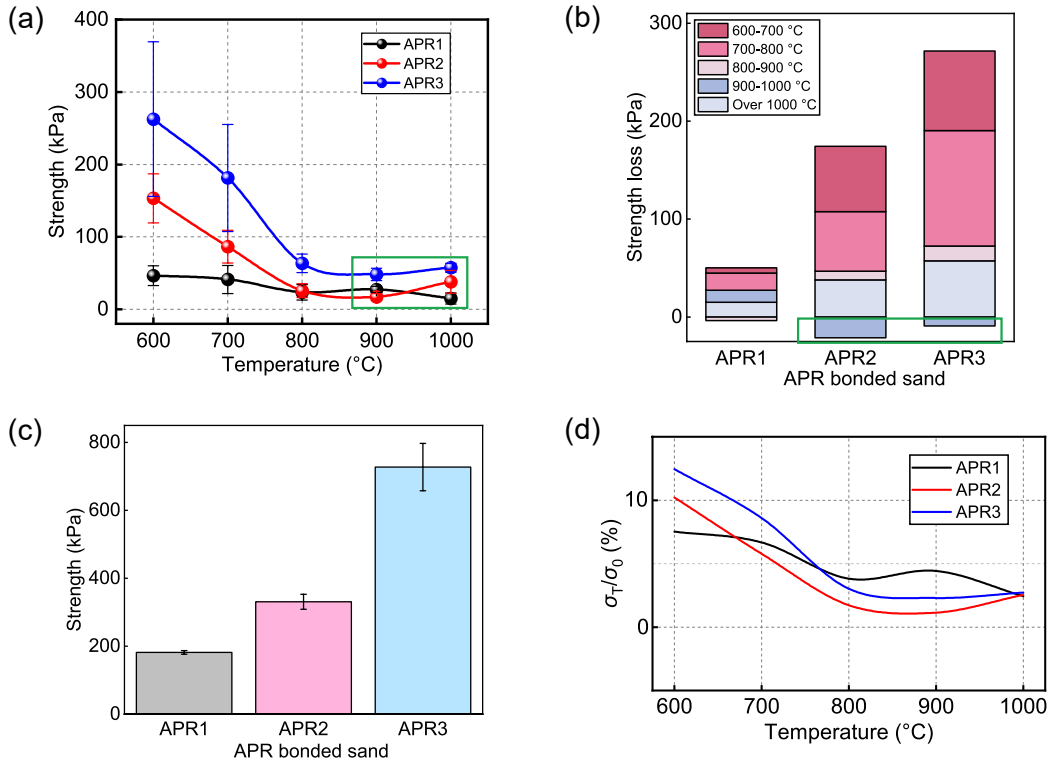

Fig. 3: Compressive strength of alkaline phenolic resin-bonded sand with three various resin contents: (a) high-temperature strength from 600 °C to 1,000 °C; (b) strength loss at different temperature gradients; (c) room temperature strength; (d) percentage of high-temperature strength (σ_T) relative to room-temperature strength (σ_0)

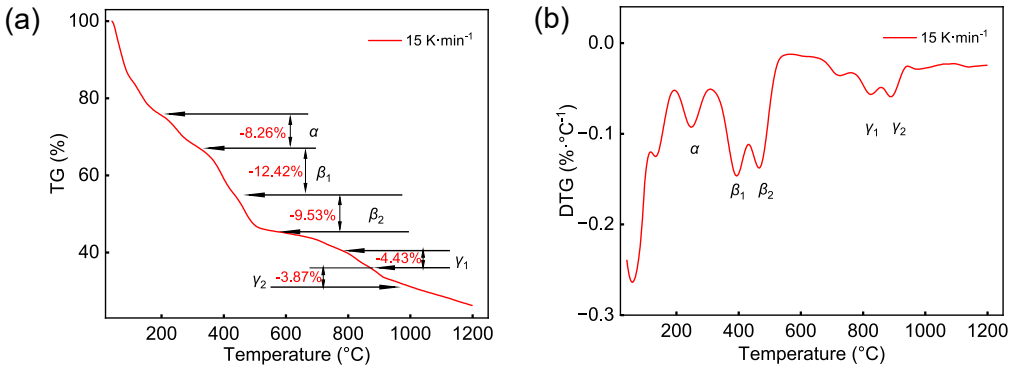

Fig. 4: TG (a) and DTG (b) results of alkaline phenolic resin[29]

Particularly noteworthy is the slight recovery in strength observed in APR2 and APR3 specimens within the 900–1,000 °C range [green boxes in Figs. 3(a) and (b)]. This phenomenon may be closely associated with the high-temperature evolution behavior of the carbon skeleton: when the temperature exceeds 900 °C, the amorphous carbon skeleton begins to undergo structural rearrangement, with some carbon atoms transitioning to the more stable sp^2 hybridized state, forming locally ordered turbostratic graphite microcrystalline structures. The growth of these carbon network planes and the increased degree of cross-linking may enhance the structural stiffness and load-bearing capacity of the carbon residue to some extent, thereby leading to the observed strength recovery instead of further decline. Meanwhile, the higher resin content provides the necessary foundation for the formation of a continuous carbon network, which explains why this phenomenon primarily occurs in APR2 and APR3. A high resin content is a prerequisite for forming a continuous and stable three-dimensional carbon network skeleton. Only when the carbon skeleton possesses sufficient continuity and structural integrity can its reorganization at high temperatures effectively translate into macroscopic strength recovery.

To further understand the relationship between initial bonding and high-temperature performance, Fig. 3(c) illustrates the room-temperature compressive strength (σ_0) of the specimens. A positive correlation is evident: σ_0 increases remarkably from approximately 180 kPa (APR1) to over 720 kPa (APR3) as the resin content rises. This substantial enhancement is primarily due to the increased volume of the binder. A higher resin content ensures a more uniform and comprehensive coating on the surface of the sand particles, leading to the formation of thicker, more numerous, and structurally sound resin binder bridges. These robust bridges establish a strong three-dimensional network at room temperature, providing exceptional initial load-bearing capacity.

Figure 3(d) plots the percentage of high-temperature strength relative to room-temperature strength (σ_T/σ_0), which serves as a critical indicator of the material's strength retention capacity during the pyrolysis process. At 600 °C, the retention rates for all specimens drop below 15%, highlighting the severe structural damage inflicted on the original polymeric network by early-stage thermal decomposition. Interestingly, APR3 exhibits a higher retention rate at 600 °C compared to APR1. The curves rapidly converge as the temperature approaches 800–850 °C, where the σ_T/σ_0 percentages all drop to a minimum of 1%–3%. This convergence suggests that in the deep pyrolysis zone, the proportional loss of strength is intrinsically governed by the thermal degradation mechanism of the alkaline phenolic resin backbone, regardless of the initial binder volume. The continuous resin films inevitably degrade into fragile carbonaceous residues, leading to a massive and uniform relative strength reduction. Furthermore, mirroring the absolute strength trend in Fig. 3(a), the σ_T/σ_0 curves for APR2 and APR3 exhibit a slight upward inflection beyond 850 °C, once again validating the strengthening effect of the carbon skeleton's sp^2 structural rearrangement at extreme temperatures.

From a practical casting perspective, this specific strength evolution profile is highly advantageous. The high room-temperature strength (σ_0) guarantees the dimensional accuracy and handling integrity of the sand molds. Concurrently, the drastic reduction in σ_T/σ_0 percentage at elevated temperatures indicates that the sand mold possesses excellent yielding behavior. This yielding is crucial for accommodating the thermal expansion of the solidifying alloy, thereby actively mitigating the constrained expansion force at the mold-metal interface and significantly reducing the risk of hot tearing defects in large or complex castings.

Conventional understanding holds that the strength of sand molds continuously degrades at high temperatures. However, this study reveals that, under certain conditions, strength recovery is possible, offering a potential new approach to actively regulating the stress state of castings during the late stages of solidification. This shift, from "passively enduring" to "active control", can significantly enhance both the academic foresight and practical relevance of the research.

3.2 Base sand types

Figures 5(a) and (b) present the high-temperature compressive strength results of alkaline phenolic resin-bonded sand prepared with three different types of base sand (grain size: 50/100) under the same resin content (APR2: 1.5wt.%), while Figs. 6(a) to (c) display the microscopic morphologies of the three base sands, respectively. Among the three base sands, both DL sand and ZZ sand are primarily composed of SiO_2, with DL sand having a higher SiO_2 content, whereas SC sand mainly consists of Al_2O_3. Additionally, the particle morphologies of DL sand and SC sand are relatively similar, both being approximately spherical, while ZZ sand exhibits more irregular particle morphology.

As shown in Fig. 5(b), specimens prepared with the three different base sands all exhibit the most significant strength loss within the 600–700 °C temperature range. This phenomenon not only further validates the conclusions regarding resin pyrolysis behavior discussed in Section 3.1, but also demonstrates that the maximum strength loss in the resin-bonded sand system is primarily determined by the thermal decomposition characteristics of the resin itself within this temperature range, showing little correlation with the type of base sand used.

It is noteworthy that specimens with ZZ sand and SC sand exhibit significant strength degradation only within the 600–700 °C range, while their compressive strength decreases only marginally above 700 °C, indicating relatively good high-temperature stability. In contrast, DL sand specimens not only undergo considerable strength loss in the 600–700 °C interval but also show noticeable additional strength reduction in the 700–800 °C range. This discrepancy may be attributed to the higher SiO_2 content in DL sand. At elevated temperatures,

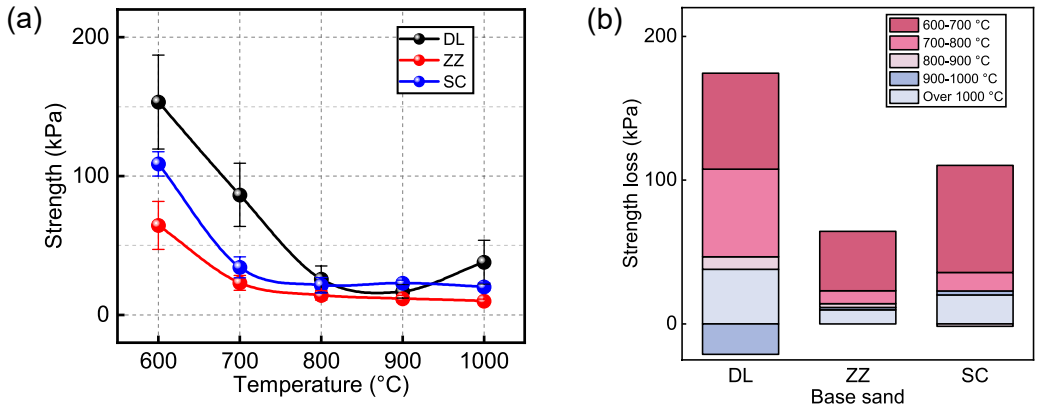

Fig. 5: Compressive strength of alkaline phenolic resin-bonded sand with three different kinds of base sand: (a) strength from 600 °C to 1,000 °C; (b) strength loss at different temperature gradients

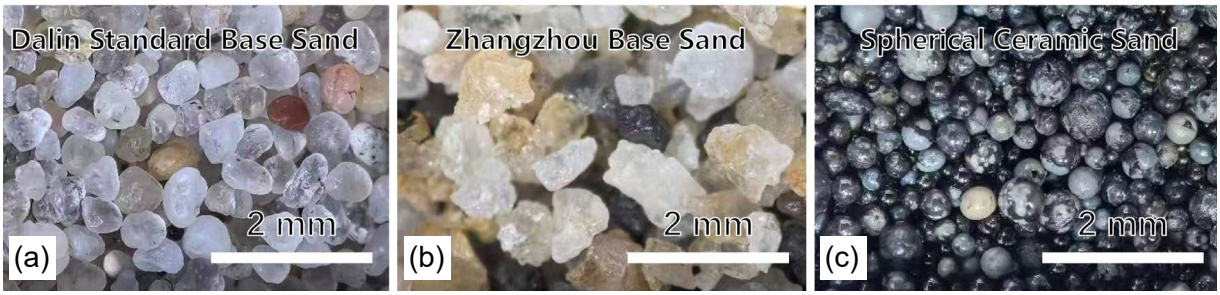

Fig. 6: Microstructure of DL (a), ZZ (b), and SC (c) sand

the crystalline transformation of SiO_2 or its interaction with residual ash may lead to further weakening of the resin bridge structure, thereby contributing to additional strength loss.

Although the pyrolysis behavior of the resin governs the primary strength loss mechanism of the resin-bonded sand system within the 600–700 °C range, the chemical composition and particle morphology of the base sand still influence the high-temperature strength evolution to some extent, particularly in terms of residual strength stability at higher temperatures.

3.3 Base sand particles size

Figures 7(a) and (b) present the high-temperature compressive strength results of alkaline phenolic resin-bonded sand prepared with the three different particle size distributions (40/70, 50/100, 70/140) of DL base sand under identical resin content. The three base sands have AFS fineness numbers of 39, 52, and 64, corresponding to coarse, medium, and fine grades, respectively. The testing methods and results for determining the AFS fineness numbers of these three base sands are provided in Tables 4, 5, and 6.

$$\eta_{40/70} = \frac{\Sigma P_n X_n}{\Sigma P_n} = 38.90 \approx 39 \tag{2}$$

$$\eta_{50/100} = \frac{\Sigma P_n X_n}{\Sigma P_n} = 52.16 \approx 52 \tag{3}$$

$$\eta_{70/140} = \frac{\Sigma P_n X_n}{\Sigma P_n} = 64.20 \approx 64 \tag{4}$$

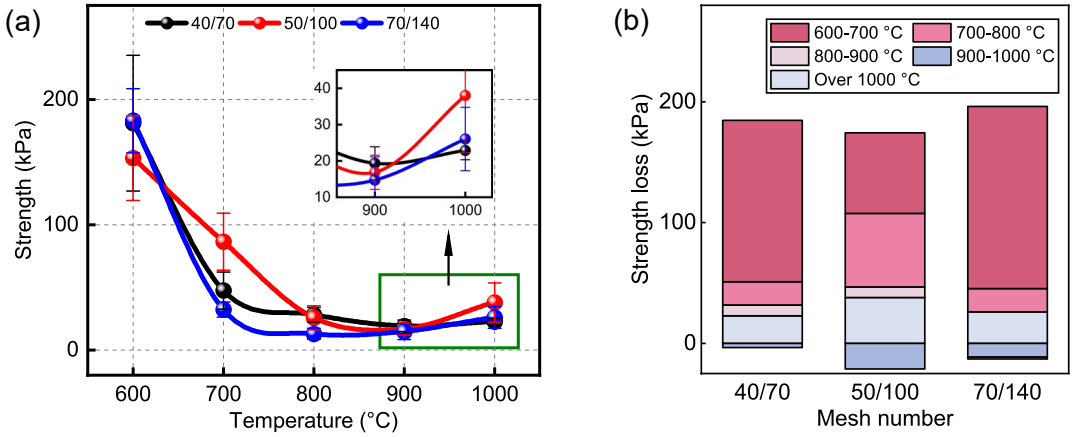

Fig. 7: Compressive strength of alkaline phenolic resin-bonded sand with three different particle size distributions: (a) strength from 600 °C to 1,000 °C; (b) strength loss at different temperature gradients

Table 4: Test results of AFS fineness number for 40/70 DL sand

Mesh number	Retained amount		Fineness factor (X_n)	Product (P_nX_n)
	Mass (g)	Mass percentage P_n (%)		
6	0	0	3	0
12	0.04	0.08002	5	0.4000
20	0.03	0.06001	10	0.6001
30	0.7	1.40028	20	28.0056
40	21.82	43.64873	30	1,309.4620
50	15.91	31.82637	40	1,273.0550
70	8.7	17.40348	50	870.1740
100	2.5	5.00100	70	350.0700
140	0.24	0.48010	100	48.0096
200	0.03	0.06001	140	8.4017
270	0	0	200	0
Pan	0	0	300	0

Table 5: Test results of AFS fineness number for 50/100 DL sand

Mesh number	Retained amount		Fineness factor (X_n)	Product (P_nX_n)
	Mass (g)	Mass percentage P_n (%)		
6	0	0	3	0
12	0.01	0.01997	5	0.0999
20	0.01	0.01997	10	0.1997
30	0.16	0.31955	20	6.3911
40	3.44	6.87038	30	206.1114
50	16.84	33.63291	40	1,345.3170
70	15.72	31.39605	50	1,569.8020
100	10	19.97204	70	1,398.0430
140	2.54	5.07290	100	507.2898
200	0.24	0.47933	140	67.1061
270	0	0	200	0
Pan	0	0	300	0

In Fig. 7(a), within the temperature range of 600 °C–900 °C, the high-temperature strength of the three specimens with different particle size distributions gradually decreases with increasing temperature, but exhibits significant differences among the various size fractions. The most critical observation is that although the fine base sand (70/140) possesses the highest initial high-temperature strength at 600 °C, its strength decreases at the fastest rate as the temperature rises, resulting in its falling below that of the medium sand (50/100) at 800 °C–900 °C. In contrast,

Table 6: Test results of AFS fineness number for 70/140 DL sand

Mesh number	Retained amount		Fineness factor (X_n)	Product (P_nX_n)
	Mass (g)	Mass percentage P_n (%)		
6	0.02	0.03997	3	0.1199
12	0.01	0.01998	5	0.0999
20	0.02	0.03997	10	0.400
30	0.06	0.11990	20	2.3981
40	0.63	1.25899	30	37.7698
50	5.52	11.03118	40	441.2470
70	15.83	31.63469	50	1,581.7350
100	20.52	41.00719	70	2,870.5040
140	7.29	14.56835	100	1,456.8350
200	0	0	140	0
270	0.04	0.07994	200	15.9872
Pan	0	0	300	0

for the coarse base sand (40/70) specimen, its smaller specific surface area allows the same amount of resin to form relatively thicker resin bridges. This bridge structure, characterized by greater "volumetric redundancy", exhibits enhanced buffering and accommodation capacity against interfacial displacements caused by thermal expansion of the silica sand particles. As a result, the strength degradation during the initial pyrolysis stage is relatively gradual, indicating better structural toughness.

Figure 7(b) further reveals the strength loss behavior of specimens with different particle sizes across high-temperature intervals. All specimens show significant strength loss in the 600 °C–700 °C range, consistent with the thermal decomposition behavior of the resin itself as discussed previously. The figure clearly demonstrates that the fine sand (70/140) experiences the most drastic strength loss within the critical 600 °C–700 °C interval, far exceeding the losses observed in the coarse and medium sands. This phenomenon may be related to the larger specific surface area of the fine sand: during the 600 °C–700 °C high-temperature interval, where the resin undergoes intense pyrolysis, the resin bridges per unit area bear a higher thermal load. This leads to a more rapid and concentrated process of destabilization and fracture, ultimately manifesting as a more substantial strength loss.

In summary, the particle size of base sand significantly influences both the high-temperature strength and strength loss behavior of alkaline phenolic resin-bonded sand. Fine sand can provide good intermediate-temperature strength, but it also undergoes the most pronounced strength degradation when passing through the critical resin pyrolysis temperature range. This finding holds important guiding significance for base

sand selection in casting production: in applications requiring guaranteed dimensional stability at high temperatures, the finest sand particles should not be selected based solely on room-temperature strength. Instead, a comprehensive consideration of their strength retention capability throughout the entire heating process is necessary. These results provide experimental evidence for optimizing base sand selection and high-temperature performance control of resin-bonded sand in casting applications.

4 Conclusions

This study systematically investigated the effects of base sand type, particle size, and resin content on the evolution of high-temperature compressive strength in alkaline phenolic resin-bonded sand. The main conclusions are as follows:

(1) Resin pyrolysis dominates the key strength loss stage. Regardless of sand type or particle size, alkaline phenolic resin-bonded sand exhibits the most significant strength loss in the 600–800 °C range, primarily due to intense thermal decomposition of the resin matrix. This indicates that the pyrolysis behavior of the resin is the controlling factor in the high-temperature strength evolution of the material.

(2) Base sand characteristics influence high-temperature strength stability. SiO_2-based sands (e.g., Dalin standard sand and Zhengzhou sand) and Al_2O_3-based sand demonstrate different strength retention capabilities at high temperatures. Sands with higher sphericity and higher SiO_2 content are more prone to additional strength loss due to crystalline transformation or interfacial reactions. The chemical composition and particle morphology of the base sand are important factors affecting strength stability above 800 °C.

(3) Base sand particle size influences strength evolution through the specific surface area effect. Particle size regulates the high-temperature strength evolution path of alkaline phenolic resin-bonded sand. Fine sand (70/140), due to its larger specific surface area, forms dense resin bridges at low temperatures, resulting in higher initial strength. However, during the main resin pyrolysis stage (600–700 °C), it exhibits the most severe strength loss due to the higher thermal load per unit area. Coarse sand (40/70) maintains consistently low strength with gradual loss. In practical selection, a balance must be struck: fine sand is suitable for scenarios requiring high strength at low-to-medium temperatures, while medium or coarse sand is more conducive to high-temperature stability control.

(4) Resin content influences the binder bridge structure and carbon skeleton evolution, further affecting high-temperature mechanical properties. A higher resin content (APR2, APR3) not only provides higher strength throughout the temperature range but also leads to a slight strength recovery in the 900–1,000 °C range. This is attributed to the structural reorganization of the carbon skeleton formed from sufficient resin pyrolysis at high temperatures, which enhances the load-bearing capacity of the residual phase. In contrast, a low resin content, for example 1.2wt.%, results in continuous strength decrease due to incomplete binder bridges.

(5) Performance in the high-temperature stage is controlled by structure of the pyrolysis residue. Above 800 °C, resin pyrolysis is essentially complete, and material properties are mainly governed by the structural characteristics of the residual carbon skeleton. Strength changes tend to stabilize in this stage, and strength recovery can even occur at very high temperatures due to changes in the carbon structure, indicating that the evolution of the carbon phase is the key to determining the performance of alkaline phenolic resin-bonded sand under extreme temperatures.

In general, this study systematically reveals the strength degradation and structural evolution mechanisms of alkaline phenolic resin-bonded sand at different temperature stages, providing a theoretical basis and experimental support for optimizing the formulation of foundry resin-bonded sands and regulating their high-temperature performance. Characterizing the precise structural evolution of the carbon residue, for instance through spectroscopic methods such as fourier transform infrared spectroscopy (FT-IR), constitutes an important direction for future research.

Acknowledgments

This work was financially supported by the National Key R&D Program of China (Grant No. 2022YFB3706802) and the National Natural Science Foundation of China (Grant Nos. 52201042 and 52435007). This work was also supported by the State Key Laboratory of Materials Processing and Die & Mould Technology, Huazhong University of Science and Technology (p2023-026).

Conflict of interest

Prof. Jian-xin Zhou is an EBM of *CHINA FOUNDRY*. He was not involved in the peer-review or handling of the manuscript. The authors have no other competing interests to disclose.

References

[1] Liu W, Yao P, and Yao S. Restraining warping of SLS sand mold via phenolic resin composites. Materials and Manufacturing Processes, 2025, 40(2): 274–283.
[2] Oguntuyi S D, Nyembwe K, Shongwe M B, et al. A review of the influence of sand properties on parts manufactured by rapid sand casting through additive manufacturing. The International Journal of Advanced Manufacturing Technology, 2025, 5–6: 1989–2002.
[3] Shi J, Shan Z, Yang H, et al. Research on frozen sand mold casting technology for complex thin-walled aluminum alloy castings. Materials Today Communications, 2024, 41: 110907.
[4] Li Y, Liu J, Zhou H, et al. Study on the distribution characteristics of microstructure and mechanical properties within the cylinder head of low-pressure sand cast aluminum alloy. International Journal of Metalcasting, 2022, 16(3): 1252–1264.
[5] Qi Y, Zhou J, Peng X, et al. A new oolitic content test method for green sand by repeated approximation. China Foundry, 2025, 22(6): 701–709.

[6] Xu Q, Zhu Y, Xu K, et al. Influences of the decomposition atmosphere and heating rate on the pyrolysis behaviors of resin sand. Buildings, 2024, 14(5): 1234.
[7] Dobosz S M, Major-Gabryś K. Strength properties of moulding sands with chosen biopolymer binders. Archieves of Foundry Engineering, 2010, 10(3): 17–20.
[8] Li Y, Zhou J, Yin Y, et al. The current application status and future prospects of resin-bonded sand process for casting in China. Foundry, 2022, 71(3): 251–270. (In Chinese)
[9] Dańko R, Kmita A, Holtzer M, et al. Development of inorganic binder systems to minimise emissions in ferrous foundries. Sustainable Materials and Technologies, 2023, 37: e00666.
[10] Khandelwal H, Ravi B. Effect of binder composition on the shrinkage of chemically bonded sand cores. Materials and Manufacturing Processes, 2015, 30(12): 1465–1470.
[11] Ren Y Y, Li Y M. Substitute materials of furfuryl alcohol in furan resin used for foundry and their technical properties. China Foundry, 2009, 6(4): 339–342.
[12] Gobinath V M, Annamalai K. Experimental investigation on chilled cast iron tappet manufacturing processes parameters. Materials and Manufacturing Processes, 2018, 33(4): 474–478.
[13] Sheikh A K, Khan M A A, Iqbal H, et al. Casting of adjuster bracket-process optimization and validation. Materials and Manufacturing Processes, 2018, 33(16): 1845–1850.
[14] Bargaoui H, Azzouz F, Thibault D, et al. Thermomechanical behavior of resin bonded foundry sand cores during casting. Journal of Materials Processing Technology, 2017, 246: 30–41.
[15] Kmita A, Fischer C, Hodor K, et al. Thermal decomposition of foundry resins: A determination of organic products by thermogravimetry-gas chromatography-mass spectrometry (TG-GC-MS). Arabian Journal of Chemistry, 2018, 11(3): 380–87.
[16] Blanco-Alegre C, Calvo A I, Castro-Sastre M Á, et al. Analysis of gaseous emission and particle number size distributions in metal casting processes with binder jetting moulds. Building and Environment, 2024, 252: 111297.
[17] Vergnano A, Facondini P, Morselli N, et al. Identification of heat transfer parameters for gravity sand casting simulations. Machines, 2024, 12(6): 414.
[18] Khorami V A. Interfacial heat transfer coefficient between sand molds and cast steel. Recent Advances in Identification, Modeling, and Control, 2026. https://doi.org/10.31224/6186.
[19] Hamadellah A, Ait el H B, Bouayad A. Hot tearing evaluation in metallic and green sand molds of $AlCu_5MgTi$ alloy. International Journal of Metalcasting, 2024, 19: 2419–2428.
[20] Wan P, Li L, Zhang L, et al. Research on testing method of resin sand high temperature compressive strength. China Foundry, 2016, 13(5): 335–341.
[21] Wang Y, Cannon F S, Li X. Comparative analysis of hazardous air pollutant emissions of casting materials measured in analytical pyrolysis and conventional metal pouring emission tests. Environmental Science & Technology, 2011, 45(19): 8529–8535.
[22] Strzemiecka B, Zieba-Palus J, Voelkel A, et al. Examination of the chemical changes in cured phenol-formaldehyde resins during storage. Journal of Chromatography: A, 2016, 1441: 106–115.
[23] Lee Y, Kim D, Kim H, et al. Activation energy and curing behavior of resol- and novolac-type phenolic resins by differential scanning calorimetry and thermogravimetric analysis. Journal of Applied Polymer Science, 2003, 89(10): 2589–2596.
[24] Ratke L, Brück S. Mechanical properties of aerogel composites for casting purposes. Journal of Materials Science, 2006, 41(4): 1019–1024.
[25] Dobosz S M, Grabarczyk A, Major-Gabryś K, et al. Influence of quartz sand quality on bending strength and thermal deformation of moulding sands with synthetic binders. Archives of Foundry Engineering, 2015, 15(2): 9–12.
[26] Stauder B J, Kerber H, Schumacher P. Foundry sand core property assessment by 3-point bending test evaluation. Journal of Materials Processing Technology, 2016, 237: 188–196.
[27] Ghosh D K. Comparison of molding sand technology between alphaset (APNB) and furan (FNB). Archives of Foundry Engineering, 2019: 11–20.
[28] González R, Colás R, Velasco A. Characteristics of phenolic-urethane cold box sand cores for aluminum casting. International Journal of Metalcasting, 2011, 5: 41–48.
[29] Peng X, Qi Y, Liu Z, et al. Toward understanding of the no-bake resin pyrolysis mechanism during sand casting process. International Journal of Metalcasting, 2025. https://doi.org/10.1007/s40962-025-01642-3.